



## Excavation-induced microseismicity: microseismic monitoring and numerical simulation\*

Nu-wen XU<sup>†1</sup>, Chun-an TANG<sup>2</sup>, Hong LI<sup>2</sup>, Feng DAI<sup>†‡1</sup>, Ke MA<sup>2</sup>, Jing-dong SHAO<sup>3</sup>, Ji-chang WU<sup>4</sup>

<sup>(1)</sup>State Key Laboratory of Hydraulics and Mountain River Engineering, College of Water Resources and Hydropower, Sichuan University, Chengdu 610065, China)

<sup>(2)</sup>Institute of Rock Instability and Seismicity Research, Dalian University of Technology, Dalian 116024, China)

<sup>(3)</sup>HydroChina Chengdu Engineering Corporation, Chengdu 610072, China)

<sup>(4)</sup>China Guodian Dadu River Dagangshan Hydropower Development Co., Ltd., Ya'an 625409, China)

<sup>†</sup>E-mail: xvnuwen@163.com; fengdai@scu.edu.cn

Received May 11, 2011; Revision accepted Sept. 23, 2011; Crosschecked May 15, 2012

**Abstract:** The volume of influence of excavation at the right bank slope of Dagangshan Hydropower Station, southwest China, is essentially determined from microseismic monitoring, numerical modeling and conventional measurements as well as in situ observations. Microseismic monitoring is a new application technique for investigating microcrackings in rock slopes. A microseismic monitoring network has been systematically used to monitor rock masses unloading relaxation due to continuous excavation of rock slope and stress redistribution caused by dam impoundment later on, and to identify and delineate the potential slippage regions since May, 2010. An important database of seismic source locations is available. The analysis of microseismic events showed a particular tempo-spatial distribution. Seismic events predominantly occurred around the upstream slope of 1180 m elevation, especially focusing on the hanging wall of fault XL316-1. Such phenomenon was interpreted by numerical modeling using RFP-A-SRM code (realistic failure process analysis-strength reduction method). By comparing microseismic activity and results of numerical simulation with in site observation and conventional measurements results, a strong correlation can be obtained between seismic source locations and excavation-induced stress distribution in the working areas. The volume of influence of the rock slope is thus determined. Engineering practices show microseismic monitoring can accurately diagnose magnitude, intensity and associated tempo-spatial characteristics of tectonic activities such as faults and unloading zones. The integrated technique combining seismic monitoring with numerical modeling, as well as in site observation and conventional surveying, leads to a better understanding of the internal effect and relationship between microseismic activity and stress field in the right bank slope from different perspectives.

**Key words:** Microseismic monitoring, Rock slope, Numerical simulation, Stability analysis, Dagangshan Hydropower Station  
**doi:**10.1631/jzus.A1100131 **Document code:** A **CLC number:** P642.22; TU45

### 1 Introduction

The rock slope stability and excavatability of rock masses are of significance problems in geotechnical engineering. This holds for both the design and construction stages. Nowadays, traditional measure-

ment techniques, such as multiple position extensometers, convergence meters, Global Positioning System (GPS) and surface subsidence monitoring, are very useful to monitor the surface deformation of rock slopes. However, it is unrealistic for them to effectively monitor the occurrence of microcrackings inside rock masses prior to the formation of a macroscopic rock fracture outside the rock slope surface. These internal microfractures may often lead to macroscopic instability failure of rock slopes. It can be concluded that there must be an intrinsic correlation

<sup>‡</sup> Corresponding author

\* Project supported by the National Natural Science Foundation of China (Nos. 50820125405, 50909013 and 50804006), and the National Basic Research Program (973) of China (No. 2007CB209404)  
 © Zhejiang University and Springer-Verlag Berlin Heidelberg 2012

between micro-fractures (microseismicity) and rock slope instability failure. It is well known that rocks loaded in a testing machine and rock masses that are stressed near underground excavations emit detectable acoustic or seismic signals. If these signals can be recorded sufficiently clearly as seismograms by a number of sensors, the original time of seismic event, its location, source parameters such as source radius and dynamic stress drop can be estimated (Mendecki, 1997; Cai *et al.*, 2001). Thus, microseismic monitoring approach has been adopted to locate such micro-fractures in rock engineering practices.

Earthquakes, with a local magnitude lower than 2.5, are called microearthquakes and are rarely felt. Microseismicity may be induced in mining areas, geothermal sites or hydroelectric reservoirs. Those microseismic activities involve changes in pore pressure, load, volume and stress, which would result in sudden shear failure in the subsurface, usually along the pre-existing weakness regions such as joints and faults. Therefore, long-term microseismic monitoring in related fields above would have the potential to reveal microcrackings geometry and to study the progressive failure of rock masses. Microseismic monitoring technique emerged from a pure research means to a mainstream industrial tool for daily safety monitoring for various geotechnical engineering during the past two decades. The approach has wide engineering applications in South Africa, Australia, Canada, Japan and North America. Some remarkable achievements have been obtained in open pit slopes (Lynch *et al.*, 2005), underground mining (Cai *et al.*, 2001; Ge, 2005; Wang and Ge, 2008; Lesniak and Isakow, 2009), oil and gas exploration fields (Li, 2009), tunnels (Hirata *et al.*, 2007), and electricity generation by hot dry rock (Tezuka and Niitsuma, 2000), etc. For example, Lynch *et al.* (2005) investigated the engineering application of microseismic monitoring in two case studies. The results showed that surface movements inferred from microseismic monitoring data enjoyed a good spatial correlation with actual surface movements. Moreover, it also showed that carefully analyzed microseismic data could be used routinely to gain greater insight into the effects of mining and subsequently can result in more accurate assessments of slopes stability. Recently, with the rapid development of Chinese economy, mines proceed to greater depth and into more com-

plex geological settings. Simultaneously, civil engineering projects, particularly large hydroelectric projects in southwest China, are being constructed. These geotechnical projects are confronted with violent rock mass failure due to deep cracks and faults, high stress levels, loose rock mass with low wave velocity, intense weathering, inter-layer extrusion zones and unloading fissures, etc. (Song *et al.*, 2011). Microseismic monitoring technique has been utilized by many researchers in such projects. For instance, in order to monitor and analyze real-time microseismicity of the left bank slope at Jinping I Hydropower Station, along Yalong River in Sichuan Province, a routine microseismic monitoring system was implemented in May, 2009 and the monitoring results can identify and delineate the rock mass failure zones and sliding surface (Xu *et al.*, 2011; 2010a). Some researchers (Zhang *et al.*, 2000; Jiang *et al.*, 2006; Li *et al.*, 2007; Yang *et al.*, 2007; Tang *et al.*, 2009) investigated the relationship between microcrackings and rock burst in deep mines, and analyzed the possibility of predicting rock burst on the rules of microfractures monitoring using different microseismic monitoring systems. Jiang *et al.* (2006), Liu *et al.* (2009), and Li and Ji (2010) also used this technique to study the failure processes of geological structures (faults, karst collapse columns) and forecast their microseismic activities associated with water inrush in underground mines. Furthermore, the technique was conducted by Tang *et al.* (2011) to predict rock bursts of the deep-buried drainage tunnels with a maximum buried depth of 2500 m in Jinping II Hydropower Station. These achievements obtained play a significant role in solving the problems of mine field stress, slope instability, hydrofracturing as well as rock burst hazards, and promote the application and development of microseismic monitoring technique worldwide. However, it is noteworthy that there are some differences between underground mines and rock slopes in using microseismic monitoring techniques. The monitoring network in the former is usually installed in different underground tunnels with great buried depths, in order to gain the understanding of the initiation, accumulation and mitigation progresses of fracture clusters due to mining-induced microseismicity. Unlike an underground mine, a rock slope has a more definite geometry, possibly lower field stress or more serious tectonic stress. The main objective of

seismic monitoring in open pit slopes is to identify and delineate real-time micro-fractures in a whole perspective view, and thus to assess the slope stability (Lynch *et al.*, 2005).

This case study is the right bank slope of Dagangshan Hydropower Station, which is located at Dadu River in Sichuan Province, southwest China (Fig. 1). The project is one of the largest scale hydroelectric constructions that are currently exploited along the mainstream of Dadu River. The dam can control a drainage area of about 62 727 km<sup>2</sup>, 81% of the total drainage area of Dadu River. It has a double-curvature dam with a maximum height of 210 m, and a total installed capacity of 2600 MW. The geological structures of this project are very complex because of the great variability in lithology and lithofacies, abutment fractures, strong weathering and widespread metamorphic terranes. The dikes, compresso-crushed zones, faults and joint fissures are developed in the dam area, such as the main dikes and faults of  $\beta_5$  ( $f_1$ ),  $\gamma_{15}$ ,  $\beta_4$ ,  $\beta_{85}$ ,  $\beta_{62}$ ,  $\beta_{83}$ ,  $\beta_{68}$ ,  $\beta_{117}$  ( $f_{78}$ ),  $\beta_{43}$ ,  $\beta_8$  ( $f_7$ ) and two deep unloading belts of XL316-1 and XL9-15. Complex geological conditions greatly affect the engineering design and construction of the project (Shao *et al.*, 2009). The layout of key water control and the right bank slope after excavation are presented in Figs. 2a and 2b, respectively (Shao *et al.*, 2006). The right bank slope of the project has complicated geological conditions such as faults, dikes, unloading cracks zones and joints with cracks development. In particular, faults X316-1 and  $f_{231}$  are the most significant factors to influence the stability of the rock slope. Weathering and unloading of rock mass inside the slope are also very serious. Natural slope surface orients 25°N–35°E and there are a variety of dikes oblique with bank slopes at a small angle. Therefore, tension fractures will easily occur at such a

shallow slope. Plenty of investigations and excavations reveal that deformation failures have superficially occurred on the slope due to stress rearrangement as a result of sapping of the River. A typical transverse section VI–VI of the right bank slope is illustrated in Fig. 2c for in-depth understanding the complexity of geological conditions (Shao *et al.*, 2006).

This study attempts to demonstrate that the microseismic activity induced by continuous excavation of the rock slope is related to the behavior of the faults in deep rock mass. The volume of influence of the working areas governs the behavior. Two significant tools have been used: microseismic monitoring and numerical simulation. By analyzing the excavation-induced microseismicity, it is possible to identify and delineate the failure zones that underlie the microseismic activity. A novel idea in the present study is to correlate microseismic monitoring records during slope excavation with other approaches including numerical modeling, conventional measurements and in situ observations. Through such a comprehensive analysis, the early warning and prevention of associated risks under difficult conditions at the right bank slope of Dagangshan Hydropower Station is proposed and implemented in this paper.

## 2 Microseismic activity and monitoring system

The microseismic monitoring network consists of Hyperion digital signal processing system, Paladin digital signal acquisition system, 24 uni-axial acceleration transducers with a natural frequency of 10 kHz installed in boreholes that drilled from sidewall of the tunnels in the right bank slope, and a 3D visualization system called microseismic monitoring



**Fig. 1 Right bank slope of Dagangshan Hydropower Station, southwest China (from Google earth)**  
(a) Overlook from whole China; (b) Dadu River at northwest China; (c) Dam site along Dadu River



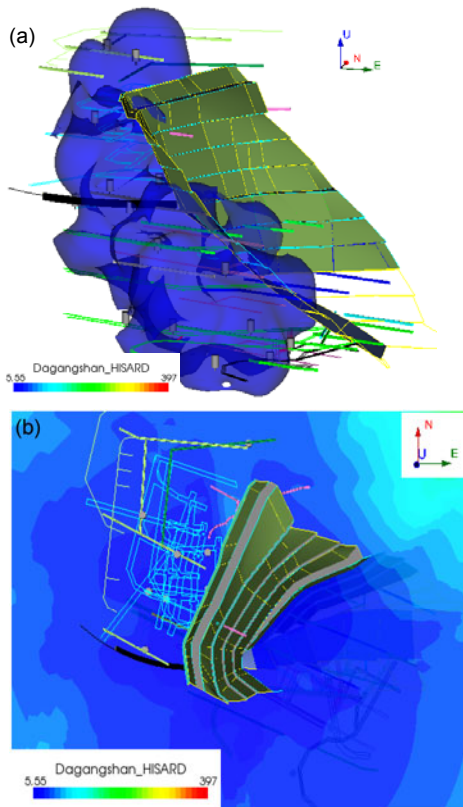


**Fig. 4** Location error analysis after optimal arrangement of sensors from a whole perspective (a) and north-easting plane looking down at 1135 m level (b). Different colors represent various seismic source location errors, the darker the color, the larger the error (Xu et al., 2010b)

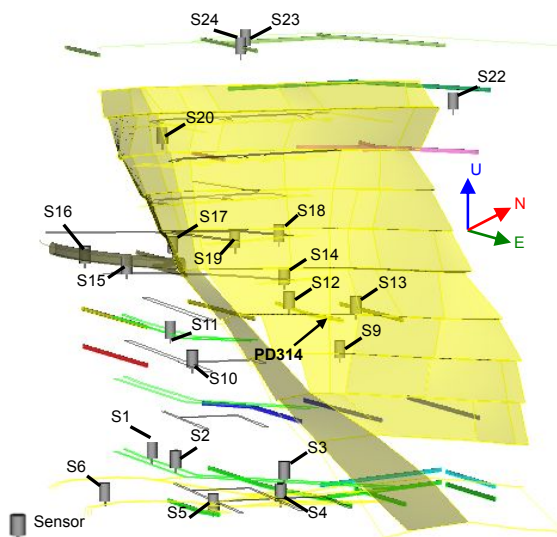


**Fig. 5** Spatial arrangement diagram of sensors at 11 elevations (Note that three sensors Nos. 7, 8, and 21 will be installed later on due to the limitation of tunnel condition. The columns present different tunnels such as transportation tunnels, drainage tunnels, and exploratory headings)

During the first half year after debugging of the system, a large number of microseismic events have been captured. The monitoring system can be operated either in automatic or manual mode to obtain related parameters of microseismic events including source locations, released energy, magnitude, apparent volume, apparent stress and seismic moment. The microseismic data recorded in the database is easy to access for generating reports by simple quarrying and for the data presentation in 3D visualization mode. Meanwhile, the contours of different seismic source location parameters for selected periods together with results of statistically analyzed data provide valuable information to understand the microcrackings behavior in deep rock mass of the slope (Urbancic and Trifu, 2000). The fundamental principle and technical parameters of microseismic monitoring technique were detailed in related studies (Urbancic and Trifu, 2000; Xu et al., 2011; 2010a).

### 3 Microseismic activity induced by continuous excavation of the rock slope

To achieve meaningful results from analysis of seismic events, the real time seismogram data itself needs to be continuously and accurately recorded for the right bank slope. Plenty of various events such as microseismic events, production blasts, and some noises subjected to different constructions and machineries, etc., are recorded here. The events with large location errors were rejected manually. The raw data recorded were saved in a database which is available for offline processing, onsets checking and further data analysis. Tempo-spatial distribution of the seismic source locations and some characteristics of microseismicity are described as follows.

#### 3.1 Temporal variation of seismic sources

After filtering out the noisy events, a dataset of 420 seismic events was recorded within a given volume of interest during the period from May 12 to Oct. 20, 2010. 48% of the database was rejected as the signals of blasting events, mechanical vibration and background noise events. The rejection criterion is that other noisy events possess their waveforms different from those of microseismic events. A plot of cumulative number of seismic events recorded from

the selected time shows one period of increased microseismic activity: July 20 to Aug. 5, 2010. This graph is compared with the time history of excavated rock mass at the bottom of the right bank slope as shown in Fig. 6. It shows that the curve of cumulative seismic events in Fig. 6a has almost the same tendency as the curve of excavated volume of rock mass (volume blasted) in Fig. 6b. This is a good correlation which illustrates a clear consistency between the volume of rock mass being excavated and the total number of seismic events. Therefore, it can be noted that excavation activities play a great role on the levels of extension fracturing within a rock slope—the deeper the slope is, the more stressed and therefore the more it fractures after being unloaded. Seismic data recorded here confirm this link, and go further by providing routine microseismic monitoring to quantify the effects that excavation is having on the slope.

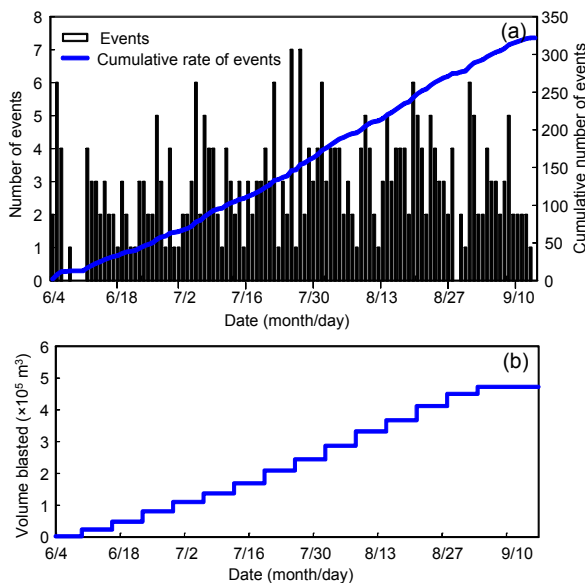


**Fig. 6** Graph of the cumulative number of microseismic events (a), and the curve of cumulative amount of rock mass removed from the right bank slope in chronological order (b). The general forms of the two graphs are similar (in 2010)

Additionally, Fig. 6a shows that the daily rate of seismic event ranges from one to seven with small bursts of activity per 5–7 d. The mean rate of events during the selected period is three per day. According to on-site investigation, swarms of microseismic events are caused by excavation-induced stress redistribution of rock masses inside the rock slope. Fig. 7 shows temporal distribution of moment mag-

nitude of microseismic events during the selected period. It shows that moment magnitude of seismic events is distributed around  $-1.2$ , which is apparently demonstrated in Fig. 8. Moreover, the frequency magnitude distribution outlines a  $b$ -value of 1.0 as the oblique line shown in Fig. 8.

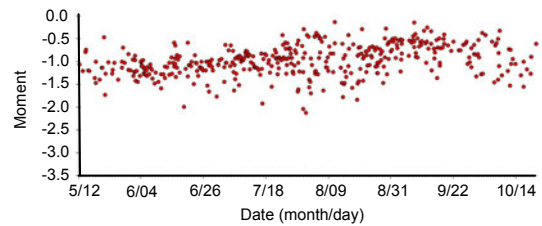


**Fig. 7** Temporal distribution of moment magnitude of microseismic events recorded during the selected period (2010)

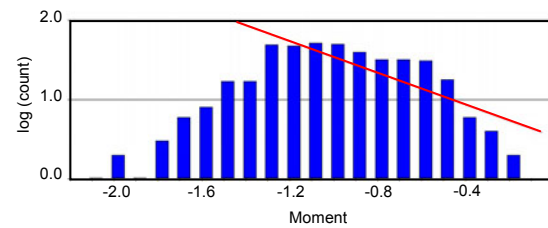


**Fig. 8** Distribution graph of moment magnitude of seismic events

### 3.2 Spatial progression of fractures

The spatial distribution of the events recorded during the selected period is shown in Fig. 9. Fig. 9a shows the absolute locations of all events including microseismic events, production blasts and some noises without manual processing. Fig. 9b shows the microseismic events recorded after eliminating interference events. During this period of microseismic monitoring, the rock slope was excavated continuously from the elevation 1070 to 980 m and shearing-resistance tunnels at 1120 and 1150 m elevation were also excavated, respectively. The microseismic events show that hypocenters are concentrated on these excavation zones and this phenomenon is due to the excavation configuration. Fig. 9 shows that seismic source locations follow the working faces and they are located where the excavation is undertaken, making it possible to correlate them unambiguously with the construction areas (Abdul-Wahed *et al.*, 2006). Therefore, the regions inside the right bank slope, where microseismicity is active or inactive, can be identified and delineated.

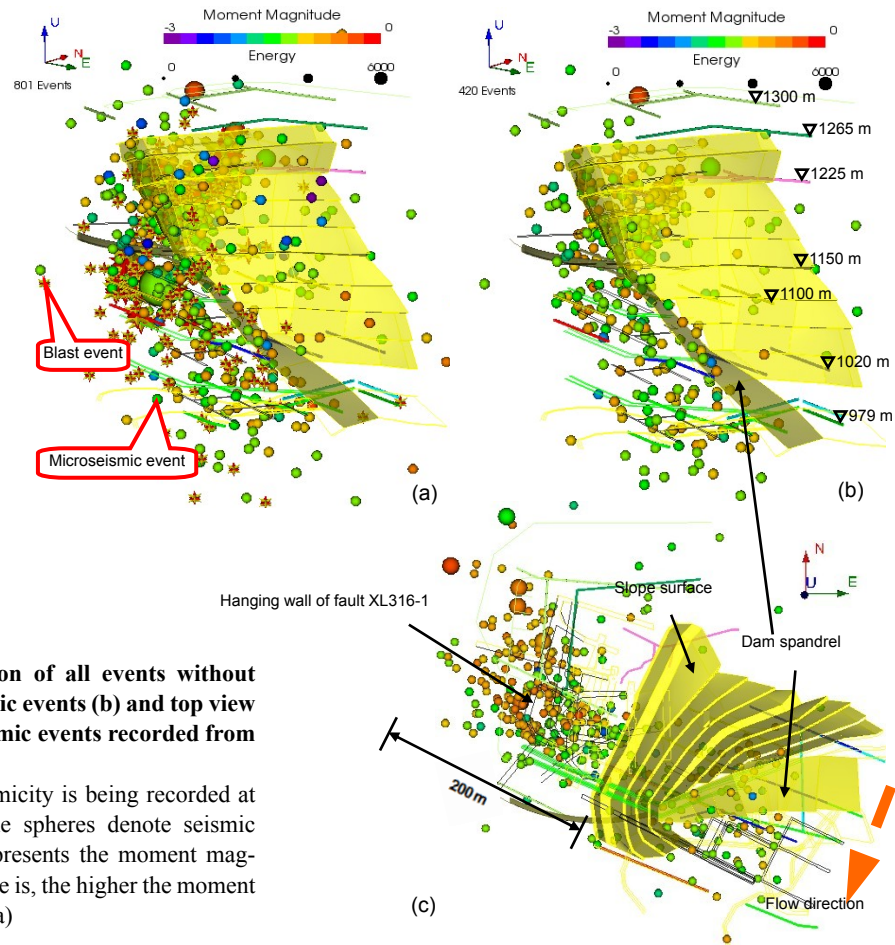


**Fig. 9** Spatial distribution of all events without processing (a), microseismic events (b) and top view from the upside (c) of seismic events recorded from May 12 to Oct. 20, 2010

It is evident that microseismicity is being recorded at significant depths here (the spheres denote seismic source locations, the size presents the moment magnitude. The bigger the sphere is, the higher the moment magnitude is, and vice versa)

In addition, Fig. 9b shows the majority of microseismic events predominantly occurred around the elevation 1180 m of the upstream slope, especially focusing on the hanging wall of the fault XL316-1 (Fig. 9c). The top view in Fig. 9c, looking from the upside, shows that the seismic events are being recorded at significant depths into the slope. However, a small number of seismic events occurred at the bottom of the rock slope. This may be partly attributed to residual movements (e.g., unloading crack zones, developed dikes and faults) inside the rock slope at high elevations and/or the excavation of shear-resistance tunnels. On the other hand, it may be also partly due to high stress concentration at the slope toe because of slope geometry. It is known that seismic activity depends on stresses and tectonic conditions, herein the tectonic stress is probably less important in this zone and the compression stress (normal stress) is higher and helps to reduce the fracturing and the seismic emission. To highlight the relationship

between spatial distribution of microseismic events and the geological structure elements, Fig. 10 shows the density contours of seismic source locations in an aerial view. Note that microseismic events show strong correlation with structure elements on-site, particularly with fault XL316-1.

### 3.3 Volume of influence

Fig. 11 shows the area map of energy loss density induced by microseismicity of the rock slope since the operation of the seismic monitoring system. It can be observed that energy loss of microseismic events induced by excavation is mostly concentrated above the elevation 1135 m of the right bank slope, with an obvious spatial distribution along faults XL316-1 and  $f_{231}$ . A small volume of energy loss by microseismicity occurred at the bottom of the right bank slope. However, the magnitude of energy loss is very small, and the potential impact on the rock slope stability needs a continuous database of seismic source locations for

in-depth investigation. With accumulation of microseismic data recorded and extension of excavation scale below 980 m level at the rock slope later on, further research on these results will be extensively studied through analysis of rock failure cases occurring in the deep rock mass. Moreover, comparison between Fig. 9 and Fig. 11 shows that seismic events mainly focused on the working zones, meaning that they can unambiguously be correlated with the advance of the rock slope excavation. This comparison shows that most of event clusters are concentrated around the construction areas.

To continuously maintain the database of seismicity such as times, locations, magnitudes, seismic moments, radiated energies, sizes and stress drops, all seismic events recorded are very desirable. Additionally, the availability of waveforms of the microseismic events recorded prior to large events and located within a few source diameters of that event would assist in back analysis and research. To study tempo-spatial changes in seismic parameters, e.g., an increase in the number of seismic events and in their

time of day distribution, a degree of acceleration in seismic deformation, a migration of density areas in energy loss of seismic events and to associate these changes with the instability of deformation within the volume of interest, the routine microseismic monitoring system should be run in real-time (Stacey *et al.*, 2004). Microseismic monitoring, which offers an efficient tool for the precise location of microfractures herein, is very helpful for identifying and delineating the microcrackings, and thus specifying the volume of influence of the right bank slope with continuous excavation in both time and space (Abdul-Wahed *et al.*, 2006). The details of instability failure mechanism of the right bank slope will be investigated in the following numerical modeling.

#### 4 Numerical simulation of the right bank slope

The main objective of numerical simulation conducted following is to better understand the behavior of the continuous excavation-induced progressive failure of the right bank slope based on field observations, mainly microseismic monitoring.

##### 4.1 Introduction of the RFPA method

A 2D finite element method (FEM)-based code called RFPA, developed by Tang and Kaiser (1998), Tang *et al.* (2000), Zhu and Tang (2006) and Zhu *et al.* (2010), was used. The RFPA can simulate the failure processes of rock mass under static or dynamic loading conditions. To simulate the failure processes, the rock medium is assumed to be composed of many mesoscopic elements whose material properties are different from one to another and are specified according to the Weibull distribution, as defined by the probability density function as follows (Li *et al.*, 2006):

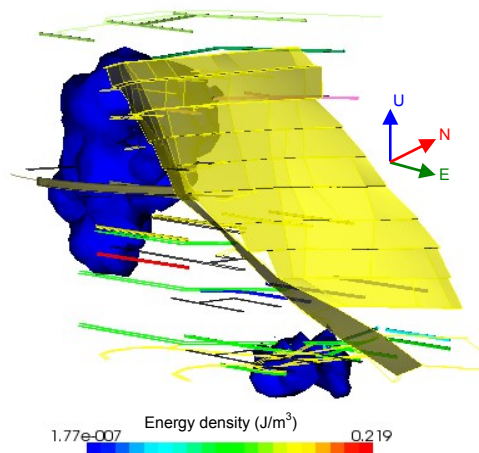


Fig. 11 Density of energy loss induced by microseismic events

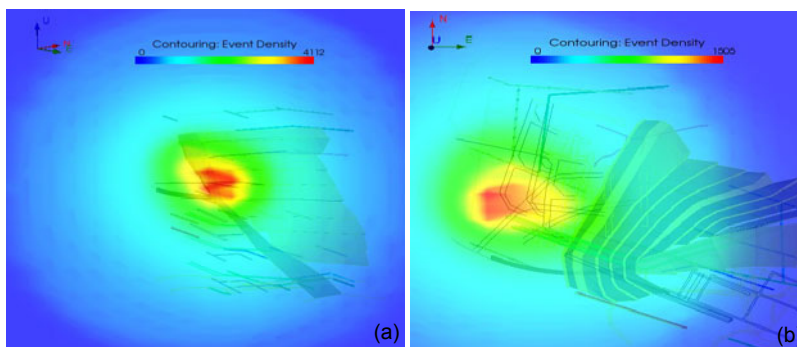


Fig. 10 Seismic source location density contours (number/m<sup>2</sup>) in northeast vertical cross-section looking north-easting (a), and north-easting plane looking down (b). The colors represent various quantities of seismic events per unit volume. The darker the color is, the larger the value of event density

$$f(u) = \frac{m}{u_0} \left( \frac{u}{u_0} \right)^{m-1} \exp\left(-\frac{u}{u_0}\right)^m, \quad (1)$$

where  $u$  is the mechanical parameter of the element (such as strength and Young's modulus). The scale parameter  $u_0$  is related to the average of the element parameters. The parameter  $m$  defines the shape of the distribution function. In RFPA<sup>2D</sup> code,  $m$  is defined as the homogeneity index of the material. Fig. 12 shows three numerical samples, which consist of 100×100 elements, generated randomly according to the Weibull distribution with different homogeneity indexes. Fig. 13 illustrates the properties of the Weibull distribution, and a larger value of  $m$  implies a more homogeneous material, and vice versa. In the definition of the Weibull distribution, the value of  $m$  must be larger than 1.0. In Fig. 12, the different degrees of grey color correspond to different magnitudes of element strength. It can be found that the strength of the elements is concentrated and close to  $u_0$  with the increase of homogeneity index. The higher homogeneity index leads to more homogeneous numerical samples. In general, it is assumed that the strength and Young's modulus conform to two individual distributions with the same homogeneity index. The Poisson's ratio usually does not vary much in reality and often is not treated with variation distributions. The computationally produced heterogeneous medium is analogous to a real specimen tested in the laboratory, therefore it is referred to as a numerical specimen in the present study (Tang *et al.*, 2000; Zhu and Tang, 2006). In addition, the FEM is applied to obtain the stress fields in the mesoscopic elements. Elastic damage mechanics is used to describe the constitutive law of the mesoscale elements when the Mohr-Coulomb criterion and the maximum tensile strain criterion are utilized as damage thresholds (Zhu and Tang, 2006; Zhu *et al.*, 2010). Detailed

descriptions on the theoretical basis and three distinctive characteristics of the code have been presented in previous studies (Tang and Kaiser, 1998; Tang *et al.*, 2000; Xu *et al.*, 2011).

Moreover, the basic principle of strength reduction method (SRM), which is an alternative approach to the failure analysis on rock or geological engineering, is adopted into the constitutive model of elements described above. The shear strength reduction technique (Matsui and San, 1992) is applied to each element. The strength  $f_0$  addressed in the constitutive model linearly degrades on the basis of the following equation:

$$f_0^{\text{trial}} = \frac{f_0}{F_s^{\text{trial}}}, \quad (2)$$

where  $F_s^{\text{trial}}$  is the trial safety efficient, and  $f_0^{\text{trial}}$  is the trial strength of element.  $f_0^{\text{trial}}$  is employed in RFPA-SRM to investigate the strength of the geological medium (in this case, the rock masses). Rock slope failure processes in this study are examined. Numerical simulation of slope stability used by RFPA-SRM is run with  $f_0^{\text{trial}}$  until the critical failure surface of the slope is determined. There are many approaches, such as non-convergence of the FEM solution and the formation of critical failure surface, etc., to define slope failure. The definition of the safety factor  $F_s$  of the slope in RFPA-SRM can be

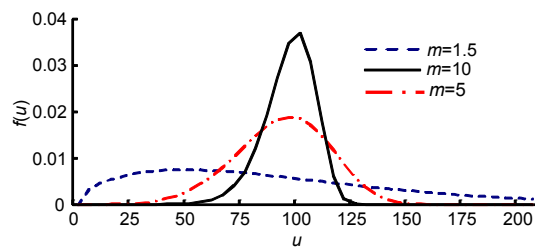


Fig. 13 Curve of different homogeneity index



Fig. 12 Numerical samples generated by RFPA<sup>2D</sup> with different homogeneity indexes  $m$

(a)  $m=1.5$ ; (b)  $m=5$ ; (c)  $m=10$

found in (Li *et al.*, 2006). The progressive failure processes of the right bank slope in Dagangshan Hydropower Station will be proposed as follows based on the SRM using RFPA<sup>2D</sup>.

**4.2 Numerical modeling and results**

A typical transverse section VI–VI of the right bank slope is obtained (Fig. 2c). The specific geometry and constraint condition for this model are shown in Fig. 14. The numerical domain of the rock slope, modeled by RFPA-SRM, has a dimension of 1400 m×720 m, and is composed of 375×180 (67 500) quadrilateral iso-parametric finite elements. The analysis is carried out under plane strain condition. The rock mass is assumed to be heterogeneous with its mechanical properties defined according to the Weibull distribution, and no heterogeneity is adopted in Poisson’s ratio and internal frictional angle. The coefficient of strength reduction is 0.05 per step. To simplify the calculation model, only main rock masses and faults are considered. The mechanical parameters of different materials are listed in Table 1 (Shao *et al.*, 2009). Note that  $E$  represents elasticity modulus,  $\mu$  means Poisson’s ratio,  $\varphi$  denotes internal friction angle, and  $c$  expresses cohesion.

Applied with the RFPA-SRM, both factor of safety ( $F_s=1.515$ ) and the corresponding shape and position of the potential sliding surface of the rock slope have been obtained. Furthermore, slope instability phenomenon was thus displayed through the progressive failure processes.

Fig. 15 demonstrates the progressive failure processes and associated acoustic emission (AE) distribution

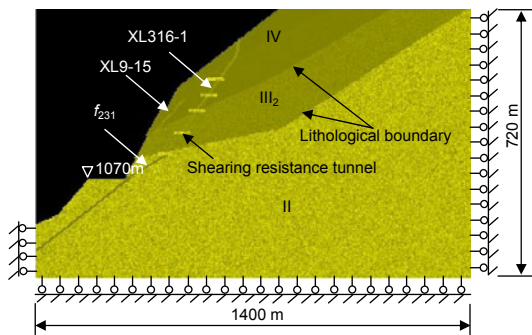


**Fig. 14 Numerical model of transverse section VI–VI of the right bank slope in Dagangshan Hydropower Station, Dadu River, Sichuan Province (the brightness of rock mass denotes the mechanical parameters such as elastic modulus and the magnitude of strength of elements, the brighter the color, the larger the value of the parameters)**

distribution of the right bank slope in Dagangshan Hydropower Station. It can be seen that the maximum shear stress firstly occurred at the bottom of the slope (step 68-11 in Fig. 15a) with rock masses strength reduction. In the wake of continuous excavation at the bottom of the slope, sliding deformation at first happens at the top of the rock slope along the hanging

**Table 1 Mechanical parameters of different materials**

Type	$E$ (GPa)	$\mu$	Shear strength		Density ( $\text{g/cm}^3$ )
			$\varphi$ ( $^\circ$ )	$c$ (MPa)	
II	18.50	0.25	52.43	2.00	2.65
III <sub>2</sub>	5.00	0.30	45.00	1.00	2.62
IV	1.25	0.35	38.65	0.70	2.58
XL316-1	0.52	0.38	27.00	0.05	2.12
XL9-15	0.61	0.34	30.20	0.06	2.06
$f_{231}$	0.48	0.38	25.00	0.08	2.20
C25	28.00	0.20	45.00	2.00	2.50

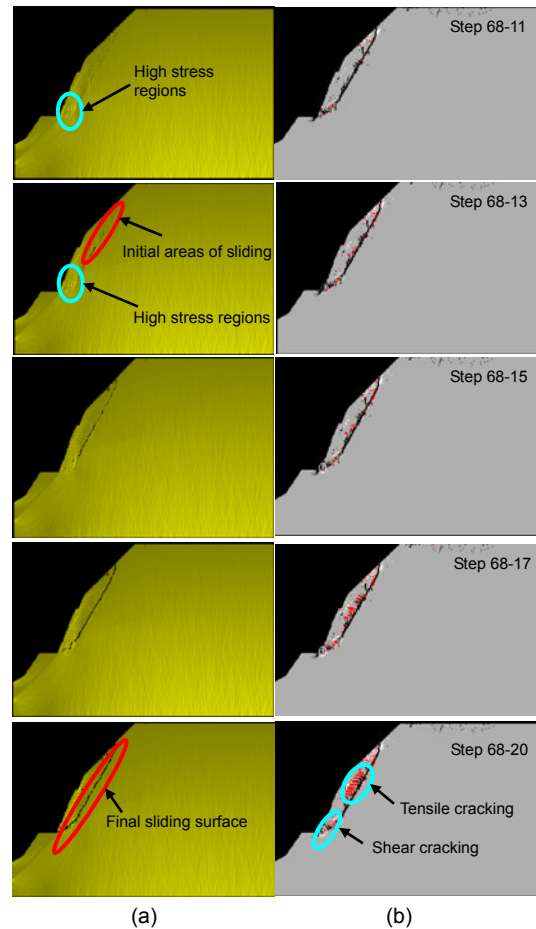


**Fig. 15 Progressive failure processes of the right bank slope based on strength reduction method using the RFPA<sup>2D</sup>. (a) Maximum shear stress; (b) AE distribution**  
The brighter the color is, the higher the shear stress

wall of fault XL316-1 (step 68-13 in Fig. 15a), then gradually extends and runs through the bottom from the top of the slope, finally leading to whole instability failure. As shown at the step 68-20 in Fig. 15b, tensile failure focuses on the top of the slope, whilst shear failure concentrates on or near the toe of the slope, accompanying high energy release. As indicated by Griffiths and Kidger (1995), both tensile and shear failures are triggered at the weakest elements, because the strength profile of the rock material is randomly distributed with specified mean and variance. Although under certain stress conditions fractures can occur in the rock mass, pre-existing fractures in the high stress zones in a slope will tend to open up. As the pre-existing joints and fractures in the high stress or stress difference zones open up due to the extension process, fractures would tend to grow into rock bridges causing microseismicity in such zones even if the magnitude of extension is not large enough to cause fresh fracturing in the rock masses (Stacey *et al.*, 2004). These can also interpret why the majority of seismic events recorded during the selected period occurs around 1150 m and higher elevations along with the main faults XL316-1 and  $f_{231}$ , but not near to the excavation faces at the bottom of the right bank slope. If the rock masses strength at the bottom of the slope cannot withstand the high stress induced by production excavation, slippage deformation of fractures will occur along the deep fissure zones from the top of the rock slope. Many microseismic events can be thus induced. The corresponding AE distribution (Fig. 15b) simulated by RFP code shows good correlation with those observed in the spatial distribution of microseismic events (Fig. 9).

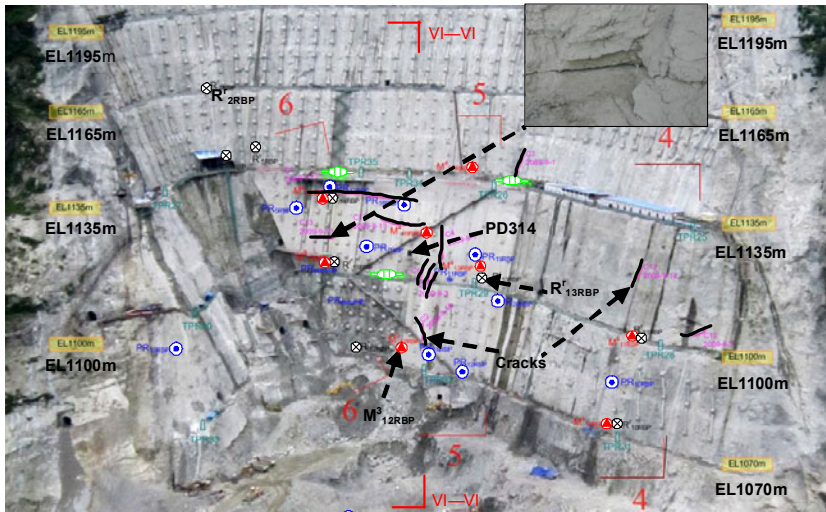
For the case study of rock slope, 2D (plane strain) modeling of the right bank slope was undertaken with the aid of a novel finite element code. The purpose of the numerical model was to investigate and model the failure mode described above and to use the model in the stability evaluation of the rock slope. The numerical analyses suggest that the observed slope behavior was a direct result of the opening up of pre-existing slope parallel fractures and joints (i.e., faults XL316-1 and  $f_{231}$ ) and the growth of these fractures and the possible formation of new fractures, which due to the fact that further extension straining of the slope face will “open up” (Stacey *et al.*, 2004).

However, the reliability of numerical modeling could just be demonstrated from a 2D perspective in the present study. It cannot replay the whole failure process of the right bank slope in an overall perspective. A 3D model should be established to make in-depth investigation on the stress distribution and failure mechanism of the rock slope. The 3D numerical results will have a noticeable and realistic comparison with the results of microseismic monitoring.

## 5 Correlation between numerical simulation, microseismic activity and routine monitoring of the rock slope

### 5.1 Routine measurement data analysis

To further analyze the correlation between routine measurement methods with microseismic monitoring, plenty of monitoring data recorded by conventional measurement techniques such as bolt stress meters, multi-point extensometers, convergence gauges and anchor stress gauges, etc., were obtained at different elevations of the right bank slope to make comparisons with the tempo-spatial distribution of seismic source locations. Fig. 16 shows the arrangement of conventional measurements apparatus and cracks distribution in the rock slope. Different symbols denote different surveying instruments. In particular the solid lines express cracks occurred in the right bank slope. These cracks were discovered in the past few months during continuous excavation of the rock slope. Noise or “bumps” in the rock slope were audible by workers in the slope. It can be obviously seen from Fig. 16 that cracks are distributed mainly around the spandrel groove slope of the arch dam, exactly above the excavation regions of the rock slope. These cracks represent an approximation of the activated volume or of the volume of influence near to the construction areas as described in Section 3.3. With respect to the depth of the seismic source locations, the microseismic monitoring study conducted at the rock slope, demonstrated that most of the seismic events may be attributed to tension fractures induced by excavation disturbance at the bottom of the slope. Fig. 17 shows the displacement processes graph of surface crackmeter at exploratory heading PD314 of the right bank slope (note that sensors Nos. 9, 12 and



⊗ Bolt stress gauge  
 ▲ Multi-point extensometer  
 ● Anchor stress gauge  
 ⇄ Clinometer  
 — Cracks on the surface of the right bank slope

**Fig. 16** Arrangement of conventional measurements apparatus and cracks distribution at the right bank slope of Dagangshan Hydropower Station

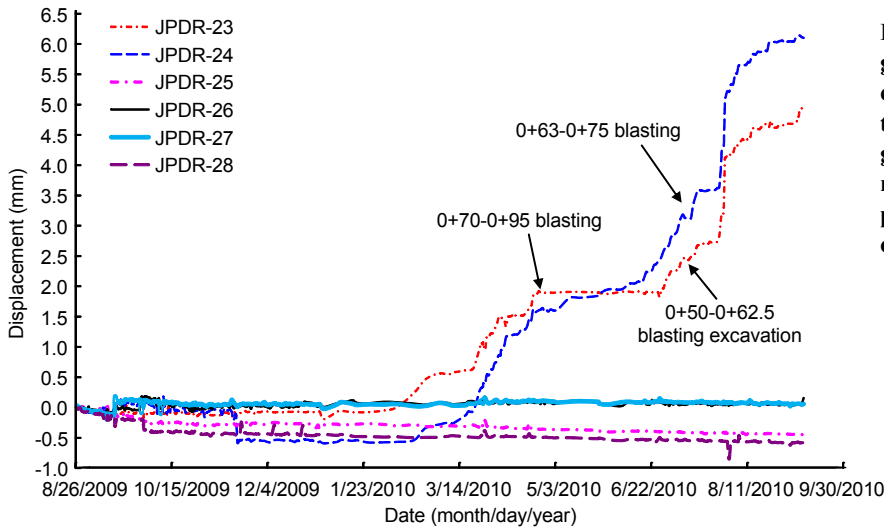


**Fig. 17** Displacement processes graph of surface crackmeter at exploratory heading PD314 of the right bank slope. The growth in data during the period of July, 2010 is a result of production blasts in the process of rock slope excavation

13 are located nearby PD314, Fig. 5). The increase of the graph during the period of July, 2010 is a result of production blasts in the process of rock slope excavation. Fig. 18 shows the displacement processes graph of graphite rod convergence gauge with six points at exploratory heading PD314 of the rock slope. Fig. 19 shows the absolute displacement processes graph of multi-point extensometer  $M^3_{12RBP}$  at dam longitudinal 0+68.5 on the elevation 1075 m of the dam foundation. Compared Figs. 17–19 and Fig. 5, a similar growth trend is obtained during the period of July, 2010, especially at the end of the month. The same change is exactly attributed to production blasts in the processes of excavation of the rock slope according to site observation and construction notes. To study the stress redistribution induced by continuous

excavation of the rock slope, stress processes graph of anchor stress gauge  $R^1_{13RBP}$  (Fig. 16) at the berm of 1101 m elevation of the right bank slope is shown in Fig. 20. It can partly reflect the stress variance of anchor cable in the deep rock masses of the rock slope. On the contrary, unlike the results of Figs. 17–19, the data of anchor stress gauge  $R^1_{13RBP}$  (Fig. 20) is decreasing during the period from May to August, 2010. This can interpret the high stress release mechanism induced by energy loss of microseismic events inside the rock slope very well. Consequently, microseismic activity can be regarded as the precursor of surface deformation and even instability failure of the rock slope. The evolutionary pattern of stress accumulation, stress releasing and stress migration in the preparation processes of potential instability disaster

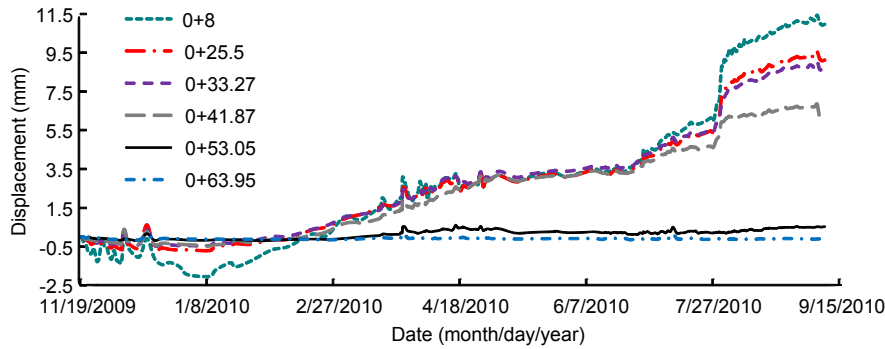


**Fig. 18** Displacement processes graph of graphite rod convergence gauge with six points at exploratory heading PD314 of the right bank slope (the numeral (e.g., 0+8) means the distances away from the adit of PD314)

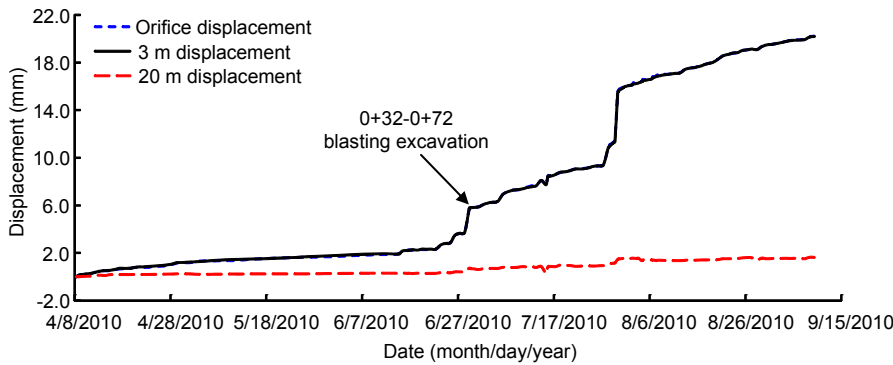


**Fig. 19** Absolute displacement processes graph of multi-point extensometer  $M^3_{12RBP}$  at dam longitudinal 0+68.5 on the elevation 1075 m of the dam foundation

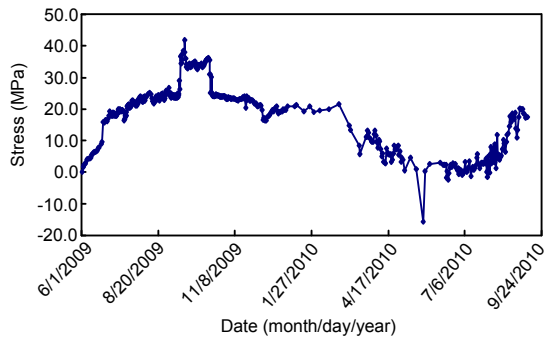


**Fig. 20** Stress processes graph of anchor stress gauge  $R^1_{13RBP}$  at the berm of 1101 m elevation of the right bank slope

is consistent with tempo-spatial distribution of microseismic events.

## 5.2 Comprehensive analysis and discussion of different data

The microseismic activity recorded during continuous excavation of the right bank slope was investigated using a microseismic monitoring technique, which was an entirely new measurement method in hydroelectric projects. Seismic events were grouped into different families such as microseismic events and production blasting events, etc., after filtering out many background noises manually (Abdul-Wahed *et al.*, 2006). The tempo-spatial distribution of the

seismic events shows that the zone affected by intense microseismic activity primarily concerns the leading edge of the excavation faces and the pre-existing joints and faults and some potential unknown geological structures (Figs. 9 and 11). This leads to the conclusion that the regions inside the right bank slope, where microseismicity is active or inactive, can be identified and delineated. Detailed analysis of high resolution seismic monitoring data from continuous excavation of the rock slope demonstrates enormous potential for using this data to track excavation propagation and to better understand the excavation process and seismic hazard in rock slopes.

As is known, the excavation of rock slope inevitably leads to stress transfer in the surrounding rock masses, in the form of either stress release or stress accumulation. Microcracking (i.e., AE) may take place in the regions of stress accumulation. The microcracking phenomenon exactly reflects the response of rock slope to stresses, or called the “outcome” of stress field. The numerical modeling used by RPEA-SRM displayed the progressive failure processes of the right bank slope successfully. Thus, the high stress field and high stress difference zones and related AE distribution of the rock slope were obtained. Comparison between Fig. 9c and Fig. 15

illustrates that microseismic events are being recorded at significant depths into the slope. Reconciliation between modeled and recorded spatial zones of high stress is important for a more complete understanding of the potential instability evolution of the right bank slope. It can be concluded that the zones identified by the location of the predominant microseismic activity are well correlated with the zones of high stress identified by numerical modeling. The most significant result is the demonstration through the location of microseismic activity and the results of numerical modeling of an extension of the stress pattern developed in the working areas.

The results from microseismic monitoring and numerical modeling are also in accordance with the interpretation stemming from in situ observations on the volume of influence induced by excavation at the bottom of the rock slope (Fig. 16). These two tools, integrating with traditional monitoring methods and in situ observation, and the correlation amongst them, are useful in explaining the behavior of potential instability mechanism of the slope. The internal effect and relationship between microseismic activity and stress field in deep rock masses of the right bank slope can thus be in-depth analyzed from different perspectives.

## 6 Conclusions

This research focuses on precisely determining the volume of influence of the right bank slope at Dagangshan Hydropower Station from the joint investigation of microseismic activity, numerical simulation, conventional measurement methods and in site observation. The following conclusions can be drawn as follows:

1. The design and installation of the microseismic monitoring system carried out at the rock slope is confirmed to be reasonable and available according to the continuous useful data recorded. As a real-time and regional technique, microseismic monitoring can not only provide invaluable information on the tempo-spatial distribution and characteristics of excavation-induced microseismicity, but also give an indication whether a particular known geological structures is seismically active or not. Planes of weakness defined by microseismic events may indi-

cate previously unknown geological structures.

2. The current microseismicity mainly occurred around the elevation 1180 m of the upstream slope, especially concentrating on the hanging wall of the fault XL316-1. This is predominantly attributed to continuous excavation of the shearing-resistance tunnels at 1120 and 1150 m elevation. Seismic source locations thus show strong correlation with structure elements on-site. Compared with conventional surveying data, it should be mentioned that excavation of the lower slope inevitably leads to stress release and migration in the surrounding rock masses, which will cause slipping deformation of the upper slope along the main faults. As a result, microcrackings (here named microseismicity) take place at the deep rock masses of upper slope.

3. Numerical modeling based on the RFPA-SRM code was performed. The progressive failure processes and associated AE distribution of a typical section VI-VI of the rock slope were obtained. Shear and tensile failures triggered at the weakest elements (i.e., faults XL316-1 and  $f_{231}$ ) are in accordance with spatial distribution of microseismic events recorded. The results of numerical simulation and microseismic monitoring are also very close to those of in situ observation and in behavior of lower slope excavation.

4. Compared with conventional measurement results, the evolutionary pattern of stress accumulation, stress releasing and stress migration in the preparation processes of potential instability disaster of the rock slope is consistent with tempo-spatial distribution of seismic source locations. Meanwhile, the usefulness of microseismic monitoring stems from the fact that microcrackings is located by the seismic monitoring system wherever they occur, and thus a 3D picture of cracks is obtained, unlike the 1D or 2D data obtained from conventional monitoring. It is not so much a short-term slope failure warning technique, but rather a system for long-term understanding of where and when rock failures are occurring in deep rock mass of the rock slope. Therefore, microseismic activity can be regarded as the precursor of surface movement and instability failure of the slope. As such, the technique may become complementary to the routine measurement techniques.

5. The presented results demonstrate that the combination of numerical simulation, microseismic monitoring, conventional surveying and in situ

observation approaches leads to a better understanding of excavation behavior of the rock slope and a more satisfactory control of the working in terms of safety in complex geological and excavation conditions.

Finally, a promising prospect that the microseismic monitoring technique will be widely used in more and more large-scale hydroelectric projects can be delineated. With the development of the methodology and technology of microseismic monitoring, the complexity of the subjects requires a commitment from the administrative departments in the form of a dedicated engineer or scientist who will operate the system. The full benefit of microseismic monitoring in rock slopes and other underground engineering is attained when this person is prepared to say 'I love my seismic system' (Mikula, 2005).

## Acknowledgements

The authors would like to thank the anonymous reviewers for their constructive comments on this paper. We are grateful to the HydroChina Kunming Engineering Corporation, China for providing valuable conventional measurement data of the project. Xiang-xi WU and Dave COLLINS in Engineering Seismology Group (ESG), Canada, are appreciated for their valuable suggestions and discussions. We also acknowledge the financial support of the Chinese Government Plan on the Recruitment of Global Young Talents and the support of Excellent Young Scholar Plan of Sichuan University, China.

## References

- Abdul-Wahed, M.K., Al Heib, M., Senfaute, G., 2006. Mining-induced seismicity: Seismic measurement using multiplet approach and numerical modeling. *International Journal of Coal Geology*, **66**(1-2):137-147. [doi:10.1016/j.coal.2005.07.004]
- Cai, M., Kaiser, P.K., Martin, C.D., 2001. Quantification of rock mass damage in underground excavations from microseismic event monitoring. *International Journal of Rock Mechanics and Mining Sciences*, **38**(8):1135-1145. [doi:10.1016/s1365-1609(01)00068-5]
- Ge, M.C., 2005. Efficient mine microseismic monitoring. *International Journal of Coal Geology*, **64**(1-2):44-56. [doi:10.1016/j.coal.2005.03.004]
- Griffiths, D.V., Kidger, D.J., 1995. Enhanced visualization of failure mechanisms by finite elements. *Computers and Structures*, **55**(2):265-268. [doi:10.1016/0045-7949(94)00440-E]
- Hirata, A., Kameoka, Y., Hirano, T., 2007. Safety management based on detection of possible rock bursts by AE monitoring during tunnel excavation. *Rock Mechanics and Rock Engineering*, **40**(6):563-576. [doi:10.1007/s00603-006-0122-7]
- Jiang, F.X., Yang, S.H., Cheng, Y.H., Zhang, X.M., Mao, Z.Y., Xu, F.J., 2006. A study on microseismic monitoring of rock burst in coal mine. *Chinese Journal of Geophysics*, **49**(5):1511-1516 (in Chinese).
- Lesniak, A., Isakow, Z., 2009. Space-time clustering of seismic events and hazard assessment in the Zabrze-Bielszowice coal mine, Poland. *International Journal of Rock Mechanics and Mining Sciences*, **46**(5):918-928. [doi:10.1016/j.ijrmms.2008.12.003]
- Li, L.C., Tang, C.A., Li, C.W., Zhu, W.C., 2006. Slope stability analysis by SRM-based rock failure process analysis (RFPA). *Geomechanics and Geoengineering*, **1**(1):51-62. [doi:10.1080/17486020600552223]
- Li, S.L., 2009. Discussion on microseismic monitoring technology and its application to underground project. *Chinese Journal of Underground Space and Engineering*, **5**(1):122-128 (in Chinese).
- Li, T., Ji, H.G., 2010. Identification of water inrush process of unknown water body using microseismic monitoring technique. *Chinese Journal of Rock Mechanics and Engineering*, **29**(1):134-139 (in Chinese).
- Li, T., Cai, M.F., Cai, M., 2007. A review of mining-induced seismicity in China. *International Journal of Rock Mechanics and Mining Sciences*, **44**(8):1149-1171. [doi:10.1016/j.ijrmms.2007.06.002]
- Liu, C., Tang, C.A., Li, L.C., Liang, Z.Z., Zhang, S.J., 2009. Analysis of probability of water inrush from grout curtain based on background stress field and microseismicity. *Chinese Journal of Rock Mechanics and Engineering*, **28**(2):366-372 (in Chinese).
- Lynch, R.A., Wuite, R., Smith, B.S., Cichowicz, A., 2005. Micro-Seismic Monitoring of Open Pit Slopes. Proceedings of the 6th Symposium on Rockbursts and Seismicity in Mines, Potvin, Y., Hudyma, M. (Eds.), Australian Center for Geomechanics, Perth, Australia, p.581-592.
- Matsui, T., San, K.C., 1992. Finite element slope stability analysis by shear strength reduction technique. *Soils and Foundations*, **32**(1):59-70. [doi:10.3208/sandf1972.32.59]
- Mendecki, A.J., 1997. *Seismic Monitoring in Mines*. Chapman and Hall, Cambridge.
- Mikula, P.A., 2005. The Practice of Seismic Management in Mines—How to Love Your Seismic Monitoring System, in Rockbursts and Seismicity in Mines. Proceedings of the 6th International Symposium, Potvin, Y., Hudyma, M. (Eds.), Australian Center for Geomechanics, Perth, Australia.
- Shao, J.D., Li, W.G., Deng, Z.W., 2006. Feasibility Study Report on Dagangshan Hydropower Station at Dadu River, Sichuan Province. Feasibility Study Report on Dagangshan Hydropower Station at Dadu River, Sichuan Province. HydroChina Chengdu Engineering Corporation, Chengdu, China (in Chinese).

- Shao, J.D., Li, W.G., Deng, Z.W., Liu, X., 2009. Engineering Geological Report on Stability Analysis of the Right Bank Slope in Dagangshan Hydropower Station at Dadu River. HydroChina Chengdu Engineering Corporation, Chengdu, China (in Chinese).
- Song, S.W., Feng, X.M., Xiang, B.Y., Xing, W.B., Zeng, Y., 2011. Research on key technologies for high and steep rock slopes of hydropower engineering in Southwest China. *Chinese Journal of Rock Mechanics and Engineering*, **30**(1):1-22 (in Chinese).
- Stacey, T.R., Wesseloo, J., Lynch, R.A., 2004. "Extension" and Seismicity in a Hard Rock Open Pit Mine. Proceedings of the 2nd International Seminar on Deep and High Stress Mining, South African Institute of Mining and Metallurgy, South Africa, p.41-53.
- Tang, C.A., Kaiser, P.K., 1998. Numerical simulation of cumulative damage and seismic energy release during brittle rock failure—Part I: Fundamentals. *International Journal of Rock Mechanics and Mining Sciences*, **35**(2):113-121. [doi:10.1016/s0148-9062(97)00009-0]
- Tang, C.A., Liu, H., Lee, P.K.K., Tsui, Y., Tham, L.G., 2000. Numerical studies of the influence of microstructure on rock failure in uniaxial compression—Part I: effect of heterogeneity. *International Journal of Rock Mechanics and Mining Sciences*, **37**(4):555-569. [doi:10.1016/s1365-1609(99)00121-5]
- Tang, C.A., Wang, J.M., Zhang, J.J., 2011. Preliminary engineering application of microseismic monitoring technique to rockburst prediction in tunneling of Jinping II project. *Journal of Rock Mechanics and Geotechnical Engineering*, **2**(3):193-208 (in Chinese).
- Tang, S.H., Pan, Y., Huang, Y.H., Ji, X.W., 2009. Application research of micro-seismic monitoring technology to geostress hazards in deep mining. *Chinese Journal of Rock Mechanics and Engineering*, **28**(Supp.2):3597-3603 (in Chinese).
- Tezuka, K., Niitsuma, H., 2000. Stress estimated using microseismic clusters and its relationship to the fracture system of the Hijiori hot dry rock reservoir. *Engineering Geology*, **56**(1-2):47-62. [doi:10.1016/S0013-7952(99)00133-7]
- Urbancic, T.I., Trifu, C.I., 2000. Recent advances in seismic monitoring technology at Canadian mines. *Journal of Applied Geophysics*, **45**(4):225-237. [doi:10.1016/s0926-9851(00)00030-6]
- Wang, H.L., Ge, M.C., 2008. Acoustic emission/microseismic source location analysis for a limestone mine exhibiting high horizontal stresses. *International Journal of Rock Mechanics and Mining Sciences*, **45**(5):720-728. [doi:10.1016/j.ijrmms.2007.08.009]
- Xu, N.W., Tang, C.A., Li, L.C., Zhou, Z., Sha, C., Liang, Z.Z., Yang, J.Y., 2011. Microseismic monitoring and stability analysis of the left bank slope in Jinping first stage hydropower station in southwestern China. *International Journal of Rock Mechanics and Mining Sciences*, **48**(6): 950-963. [doi:10.1016/j.ijrmms.2011.06.009]
- Xu, N.W., Tang, C.A., Sha, C., Liang, Z.Z., Yang, J.Y., Zou, Y.Y., 2010a. Microseismic monitoring system establishment and its engineering applications to left bank slope of Jinping I Hydropower Station. *Chinese Journal of Rock Mechanics and Engineering*, **29**(5):915-925 (in Chinese).
- Xu, N.W., Tang, C.A., Wu, S.H., Li, G.L., Yang, J.Y., 2010b. Optimal design of microseismic monitoring networking and error analysis of seismic source location for rock slope. *Advanced Materials Research*, **163-167**:2991-2999.
- Xu, N.W., Tang, C.A., Wu, S.H., Li, G.L., Yang, J.Y., Cheng, B., 2010c. Application of microseismic monitoring technique in the right bank slope of Dagangshan Hydropower Station. *Journal of Disaster Prevention and Mitigation Engineering*, **30**(Supp.):216-221 (in Chinese).
- Yang, C.X., Luo, Z.Q., Tang, L.Z., 2007. Study on rule of geostatic activity based on microseismic monitoring technique in deep mining. *Chinese Journal of Rock Mechanics and Engineering*, **26**(4):818-824 (in Chinese).
- Zhang, X.M., Yu, K.J., Xi, J.D., Kong, F.M., Zhang, X.B., Wang, S.J., 2000. Research and application of microseismic technology to fractured mine and caving zones monitoring. *Journal of China Coal Society*, **25**(6): 566-569 (in Chinese).
- Zhu, W.C., Tang, C.A., 2006. Numerical simulation of Brazilian disk rock failure under static and dynamic loading. *International Journal of Rock Mechanics and Mining Sciences*, **43**(2):236-252. [doi:10.1016/j.ijrmms.2005.06.008]
- Zhu, W.C., Li, Z.H., Zhu, L., Tang, C.A., 2010. Numerical simulation on rockburst of underground opening triggered by dynamic disturbance. *Tunnelling and Underground Space Technology*, **25**(5):587-599. [doi:10.1016/j.tust.2010.04.004]